5-2016

# Turning Performance in Squid and Cuttlefish: Unique Dual-Mode, Muscular Hydrostatic Systems

Rachel A. Jastrebsky
*Old Dominion University*

Ian K. Bartol
*Old Dominion University*, ibartol@odu.edu

Paul S. Krueger

Follow this and additional works at: https://digitalcommons.odu.edu/biology_fac_pubs

Part of the Biomechanics Commons, and the Marine Biology Commons

*The Company of*
**Biologists**

# RESEARCH ARTICLE

# Turning performance in squid and cuttlefish: unique dual-mode, muscular hydrostatic systems

Rachel A. Jastrebsky[1,*], Ian K. Bartol[1] and Paul S. Krueger[2]

## ABSTRACT

Although steady swimming has received considerable attention in prior studies, unsteady swimming movements represent a larger portion of many aquatic animals' locomotive repertoire and have not been examined extensively. Squids and cuttlefishes are cephalopods with unique muscular hydrostat-driven, dual-mode propulsive systems involving paired fins and a pulsed jet. These animals exhibit a wide range of swimming behavior, but turning performance has not been examined quantitatively. Brief squid, *Lolliguncula brevis*, and dwarf cuttlefish, *Sepia bandensis*, were filmed during turns using high-speed cameras. Kinematic features were tracked, including the length-specific radius of the turn ($R/L$), a measure of maneuverability, and angular velocity ($\omega$), a measure of agility. Both *L. brevis* and *S. bandensis* demonstrated high maneuverability, with $(R/L)_{min}$ values of $3.4\times10^{-3}\pm5.9\times10^{-4}$ and $1.2\times10^{-3}\pm4.7\times10^{-4}$ (mean±s.e.m.), respectively, which are the lowest measures of $R/L$ reported for any aquatic taxa. *Lolliguncula brevis* exhibited higher agility than *S. bandensis* ($\omega_{a,max}$=725.8 versus 485.0 deg s$^{-1}$), and both cephalopods have intermediate agility when compared with flexible-bodied and rigid-bodied nekton of similar size, reflecting their hybrid body architecture. In *L. brevis*, jet flows were the principal driver of angular velocity. Asymmetric fin motions played a reduced role, and arm wrapping increased turning performance to varying degrees depending on the species. This study indicates that coordination between the jet and fins is important for turning performance, with *L. brevis* achieving faster turns than *S. bandensis* and *S. bandensis* achieving tighter, more controlled turns than *L. brevis*.

KEY WORDS: Locomotion, *Lolliguncula brevis*, *Sepia bandensis*, Maneuverability, Agility, Biomechanics, Swimming

## INTRODUCTION

Many studies on aquatic locomotion have focused on steady rectilinear swimming of fishes (Bartol et al., 2008; Blake et al., 1995; Domenici and Blake, 1991, 1997; Drucker and Lauder, 1999, 2000; Gray, 1933; Harper and Blake, 1990; Kasapi et al., 1993; Liao et al., 2003; Maia and Wilga, 2013; Webb, 1975, 1978, 1983; Wilga and Lauder, 2000), cephalopods (Anderson and Grosenbaugh, 2005; Bartol et al., 2001a,b, 2008, 2009a,b, 2016; O'Dor, 1988; Stewart et al., 2010; Wells and O'Dor, 1991) and marine mammals (Fish, 1993, 1994; Fish et al., 2008). Although these studies have provided valuable information on swimming performance, much less is known about unsteady and intermittent swimming movements. Unsteady mechanisms comprise a significant portion of the locomotive repertoire for most aquatic taxa and are ecologically important for capturing prey, eluding predators and navigating through complex habitats (Webb, 1983; Weihs, 1972, 1993).

Two important parameters for assessing unsteady motions are maneuverability and agility. Maneuverability is the ability to turn in a confined space, and is defined as the length-specific radius of the turning path ($R/L$), where $R$ is the radius of the turning path and $L$ is total body length (Walker, 2000). Agility is the rate of turning, and is defined as the average and maximum angular velocity, $\omega_{avg}$ and $\omega_{max}$, during turning (Norberg and Rayner, 1987; Webb, 1994). Exceptional turning performance is characterized by a swimmer's ability to exhibit both high agility and high maneuverability (Norberg and Rayner, 1987; Webb, 1994).

The role of body flexibility in turning performance has been considered in a variety of aquatic taxa, and aquatic animals are often placed in three general classifications: (1) flexible-bodied, (2) stiff-bodied and (3) rigid-bodied. These classifications derive from Webb (1984) and relate to transient and sustained swimming preferences. Flexible-bodied animals include many species of ray-finned fishes, some smaller sharks and some marine mammals, such as sea lions (Fish, 2002; Fish et al., 2003; Maresh et al., 2004; Webb, 1984). Paired fins/appendages are generally present and help to control turns in these flexible-bodied nekton (Webb, 1984). Stiff-bodied animals, including large cetaceans and thick-skinned tuna, tend to be streamlined and have a stiff body with a deep, narrow caudal fin. This body form maximizes thrust while reducing drag (Blake et al., 1995; Fish, 2002; Webb, 1984). Finally, rigid-bodied animals are not able to bend their body axis significantly because of the presence of an exoskeleton, hard carapace or internal shell, and include animals such as boxfish, aquatic beetles and aquatic turtles. Highly flexible-bodied animals, such as sea lions, spiny dogfish and knifefish, tend to achieve not only greater maneuverability than stiff-bodied and rigid-bodied animals, but also greater agility (Domenici and Blake, 1997; Domenici et al., 2004; Fish et al., 2003). This is not surprising given that more rigid bodies limit body axis bending, precluding turning effectively in tight spaces (limiting maneuverability) and restricting the ability to reduce the body's second moment of inertia about the dorsoventral rotational axis, resulting in high inertial resistance to rotation (limiting agility) (Walker, 2000). Rigid bodies also result in relatively high pressure drag resisting rotation because the angle of attack of the body and local flow is close to 90 deg along the length of the body (Walker, 2000).

Though it seems reasonable to conclude that more rigid-bodied nekton have limited maneuverability and agility relative to flexible-bodied nekton as stated above, certain studies reveal that this is not always the case. For example, boxfishes, which have two-thirds to three-quarters of their bodies encased in a rigid carapace, are highly maneuverable relative to flexible-bodied animals, but not very agile (Blake, 1977; Walker, 2000). The high level of maneuverability

[1]Department of Biological Sciences, Old Dominion University, Norfolk, VA 23529, USA. [2]Department of Mechanical Engineering, Southern Methodist University, Dallas, TX 75275, USA.

*Author for correspondence (rwigt001@odu.edu)

**List of symbols and abbreviations**

| | |
|---|---|
| COR | center of rotation |
| $D_{max}$ | maximum distance between the COR at any two instances during the turning sequence |
| DML | dorsal mantle length |
| $L$ | total body length |
| $R$ | radius of the turning path |
| $(R/L)_{a,min}$ | absolute minimum length-specific turning radius using a 90% cut-off |
| $(R/L)_{mean}$ | mean length-specific turning radius |
| $(R/L)_{min}$ | minimum length-specific turning radius using a 90% cut-off averaged over all turning sequences |
| $\theta_{lam}$ | lateral angle between the arms and mantle |
| $\theta_{lmh}$ | lateral angle between the mantle and the horizontal |
| $\theta_v$ | ventral angle between the arms and mantle |
| $\theta_{v,mean}$ | mean ventral angle between the arms and mantle |
| $\theta_{v,min}$ | minimum ventral angle between the arms and mantle |
| $\theta_{total}$ | total angular displacement |
| $\omega_{a,max}$ | absolute maximum angular velocity |
| $\omega_{avg}$ | mean angular velocity |
| $\omega_{max}$ | maximum angular velocity averaged over all turning sequences |

derives from their ability to rotate along a tight vertical axis using oscillating and undulating movements of the pectoral, dorsal and anal fins, while the caudal fin acts as a rudder (Blake, 1977; Walker, 2000). The whirligig beetle is another rigid-bodied swimmer, but unlike boxfish, it is highly agile with limited maneuverability. Whirligig beetles use asymmetrical paddling motions of the outboard legs to turn as well as abduction of the inboard elytra (a modified, hardened forewing) and sculling of the wing (Fish and Nicastro, 2003). Rivera et al. (2006) investigated turning performance in the painted turtle, *Chrysemys picta*, another rigid-bodied swimmer, and found that it is relatively similar to the boxfish in terms of maneuverability. However, the turtle's shell morphology and limb positioning facilitates greater agility than that observed in boxfish.

Cuttlefishes and squids are unique in that they do not fall neatly into any of the three body categories described above. Squids and cuttlefishes possess structures (chitinous pen or cuttlebone, respectively) that limit appreciable longitudinal length changes and bending along the mantle, much like the carapace of a rigid-bodied boxfish. However, the arms, which extend outward from the head and comprise a significant portion of total body length, are highly flexible, even to a higher degree than the bodies of flexible-bodied nekton.

An additional distinction is that cuttlefishes and squids use two fundamentally distinct propulsors for turning (fins and jet) and have a number of control surfaces (fins and keeled arms). The dual mode system of a pulsed jet and paired fins is powered by muscular hydrostats, or tightly packed, three-dimensional muscular arrays that lack hardened skeletal support elements (Kier et al., 1989). The pulsed jet is generated in two phases, an inhalant and exhalant phase. During the inhalant phase, radial expansion of the mantle causes an inflow of water into the mantle cavity through intakes located at the anterior portion of the mantle (O'Dor, 1988). During the exhalant phase, circular muscles in the mantle contract, decreasing mantle circumference and increasing the pressure in the mantle cavity. The increase in pressure closes the slots at the anterior intakes so that the water in the mantle cavity is forced out through the funnel, producing a thrust force that propels the cephalopod (Anderson and DeMont, 2000; Bartol et al., 2008, 2009b; Thompson and Kier, 2001). The funnel is flexible and can

be rotated within a hemisphere below the body, allowing the animal to move backwards, forwards, upwards and sideways depending on the trajectory of the jet (Boyle and Rodhouse, 2005). The fins of squid and cuttlefish move in complex patterns ranging from undulatory waves to pronounced flaps to produce thrust, maintain stability and provide lift (Bartol et al., 2001a,b, 2016; Hoar et al., 1994; Kier et al., 1989; Stewart et al., 2010). Cuttlefish can produce undulatory fin waves in opposite directions on each side of the body and generally rely more heavily on their fins for locomotion compared with squid (Hoar et al., 1994). The cuttlebone of cuttlefishes allows them to regulate and achieve desired buoyancy levels (Denton and Gilpin-Brown, 1961), a mechanism that is absent in most squids. In fact, many inshore, coastal squid species, such as *Lolliguncula brevis*, are negatively buoyant and must expend energy swimming to remain at a position in the water column (Bartol et al., 2001a,b). Given their distinct body flexibility and propulsion system characteristics, squids and cuttlefishes represent a unique group for comparison with previously studied nekton.

This study aims to investigate turning performance of two cephalopod species with very different morphologies and locomotory strategies than previously studied aquatic animals. The two species considered here are the coastal inshore squid species *L. brevis*, and the tropical coastal cuttlefish species *Sepia bandensis*, which differ morphologically and physiologically. The paired fins of *L. brevis* are relatively short and rounded, and the fins of *S. bandensis* extend along the length of the mantle, though they are not especially broad in span. *Lolliguncula brevis* is negatively buoyant and must expend considerable energy maintaining position in the water column (Bartol et al., 2001a,b), whereas *S. bandensis* uses an internal cuttlebone to maintain neutral buoyancy, which reduces energetic costs associated with vertical positioning (Denton and Gilpin-Brown, 1961). Moreover, *S. bandensis* relies more extensively on their fins for locomotion than *L. brevis*. Given that *S. bandensis* has longer fins than *L. brevis* and is neutrally buoyant, characteristics that presumably favor turning control, we expect *S. bandensis* will have higher maneuverability than *L. brevis*. However, the more powerful jets of squid relative to cuttlefish should translate to an advantage in agility for *L. brevis* compared with *S. bandensis*. The unique body architecture of squid and cuttlefish, which includes a vectored jet and highly flexible fins for active, controlled turning and arms for ruddering and positional control, also may provide distinct advantages in turning performance relative to other nekton. Therefore, we predict that both squid and cuttlefish will exhibit higher maneuverability and agility than other nekton considered to date, especially classical rigid-bodied swimmers.

## MATERIALS AND METHODS

The animals used for this study were the dwarf cuttlefish, *Sepia bandensis* Adam 1939, and the brief squid, *Lolliguncula brevis* (Blainville 1823). The dorsal mantle length (DML) of *L. brevis* individuals ranged from 3.2 to 7.4 cm (mean±s.d.=5.5±1.2 cm). The total length ($L$), including the arms, ranged from 4.8 to 11.9 cm (mean=9.03±2.02 cm). The mantle, on average, made up 61.5±2.8% of the total body length. The DML of *S. bandensis* individuals ranged from 2.5 to 3.8 cm (mean=3.1±0.5 cm), and $L$ ranged from 4.5 to 6.9 cm (mean=5.7±0.9 cm). The mantle, on average, made up 55.5±1.9% of the total body length. *Sepia bandensis* were purchased from a commercial supplier (Consistent Sea Inc., Gardena, CA, USA) and were kept individually in submerged plastic buckets (36 cm deep and 30 cm wide) with

drilled 6 cm diameter holes and mesh liners for water circulation. The buckets floated freely in a recirculating 450 gallon seawater system at a salinity of 33–35 ppt, a temperature of 24–25°C and a pH of 8.0–8.2. Ammonia levels were kept below 0.2 ppm. *Lolliguncula brevis* were caught by trawl net at the Virginia Institute of Marine Science Eastern Shore Marine Lab, Wachapreague, VA, USA, and were transported back to Old Dominion University in aerated livewells. The adults were maintained in a 450 gallon recirculating seawater system (separate from the cuttlefish system) at a salinity of 25–30 ppt, a temperature of 15–21°C and a pH of 8.0–8.2. Ammonia levels again were kept below 0.2 ppm and a moderate current was generated in the *L. brevis* holding tank to facilitate active swimming. Both species were fed a diet of live grass shrimp (*Palaemonetes pugio*).

A Plexiglas viewing chamber measuring 30.5×30.5×25.4 cm was placed on a stand that allowed unobstructed viewing from both lateral and ventral perspectives. The chamber was filled with seawater of the same salinity and temperature as the holding tanks. The water in the chamber was aerated overnight prior to conducting trials. The chamber was illuminated with five 500 W lights outfitted with color gel #27 filters (transmit wavelengths >600 nm), as red light tended to reduce stress on the animals compared with full spectrum illumination. For each trial, the cuttlefish or squid was placed in the chamber and allowed to acclimate for at least 5 min prior to recording. Turns either occurred naturally without any experimental intervention or, in cases where the cephalopods would not turn consistently, were elicited by simulating predatory behavior. Simulating predatory behavior was accomplished by tying a grass shrimp to a piece of tubing and moving the tubing in gentle circular motions in the chamber. Trials were terminated if the animal became unresponsive or caught the shrimp. Data from five *S. bandensis* (2.5–3.8 cm DML, mean=3.1±0.5 cm) and 14 *L. brevis* (3.2–7.4 cm DML, mean=5.5±1.2 cm) were collected, with three to 15 turning sequences per animal being considered for further analyses.

The turns were recorded using two synchronized high-speed DALSA Falcon video cameras (1400×1200 pixel resolution; DALSA, Waterloo, ON, Canada) positioned ventrally and laterally to the viewing chamber. The ventral camera was fitted with a 25 mm lens and the lateral camera was fitted with a 35 mm lens (Fujinon TV Lens, Fujinon Corporation, China). The high-speed cameras were triggered by the onboard counter on two CLSAS capture cards (IO Industries, London, ON, Canada) to capture video at 100 frames $s^{-1}$. Video frames from the DALSA cameras were transferred to hard disk in real time using the two CLSAS capture cards and Streams 5 software (IO Industries).

Frame-by-frame position tracking of the cephalopod body features was accomplished using image tracking software (Hedrick, 2008). Seven points were tracked in the ventral view: (1) tail tip, (2) funnel base, (3) arm tip, (4) mantle right side (midway along length of mantle), (5) mantle left side (midway along length of mantle), (6) right fin tip (at maximum chord point) and (7) left fin tip (at maximum chord point) (Fig. 1B). Six points were tracked in the lateral view: (1) tail tip, (2) eye, (3) arm tip, (4) proximal funnel opening, (5) distal funnel opening and (6) fin tip (maximum chord point) (Fig. 1A). The tracked points in the ventral view were used to determine: (1) the center of rotation (COR), (2) angular velocity, (3) total angular displacement ($\theta_{total}$), (4) direction of the turn, (5) time to execute the turn, (6) angle between the mantle and arms ($\theta_v$), (7) frequency of fin beats and (8) mantle diameter. $\theta_v$ is defined as the angle between the arms and the mantle in the ventral perspective; we report a mean angle throughout the turn, $\theta_{v,mean}$, and an absolute
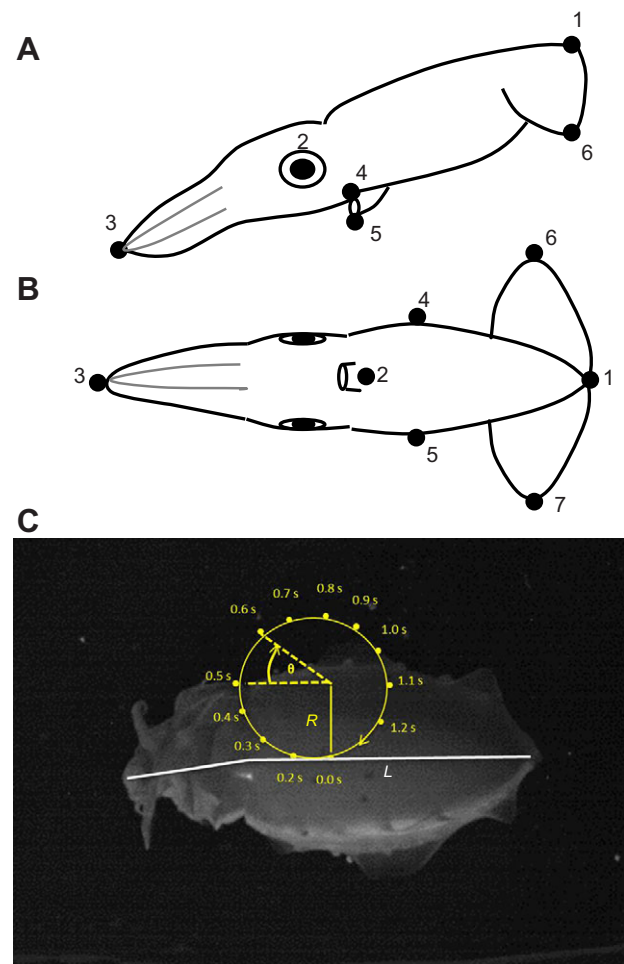


**Fig. 1. Points tracked in the lateral and ventral views.** (A) Points tracked in the lateral view for *Lolliguncula brevis*: (1) tail tip, (2) eye, (3) arm tip, (4) funnel opening top, (5) funnel opening bottom and (6) fin tip. (B) Points tracked in the ventral view for *L. brevis*: (1) tail tip, (2) funnel base, (3) arm tip, (4) mantle right, (5) mantle left, (6) fin tip right and (7) fin tip left. The same points were tracked for *Sepia bandensis*. (C) Center of rotation (COR) points are shown for a hypothetical turn where the cuttlefish is turning clockwise with time (COR points are displayed per 0.1 s). The radii (R) of the COR points are measured and divided by the total length of the animal (L, white line segments) to calculate length-specific radii of the turns (R/L). The angle that the animal moved (θ) between COR points was divided by the time difference between measurements (Δt) to determine angular velocities (ω).

minimum angle during the turn, $\theta_{v,min}$ (Fig. 2), both averaged over all turning sequences. The mantle diameter was determined for *L. brevis* only, as the cuttlebone in *S. bandensis* limits visible changes in the ventral view.

The data were smoothed using the cross-validation criterion. This smoothing method uses smoothed splines where the level of smoothing is determined such that the root-mean-squared error of the splines determined with points from the data individually excluded is minimized (Walker, 1998). In the present implementation, the minimization is determined to within 0.1% of the actual minimum to speed convergence of the method.

The COR was the point in the ventral view that moved the least during the turn. Finding the COR was performed using an in-house MATLAB code that either used the line segment connecting the tail tip to the funnel base, or used a two segment approach with the lines connecting the tail tip to the funnel base and then the funnel base to the arm tip. The code was generalized so that the COR did not
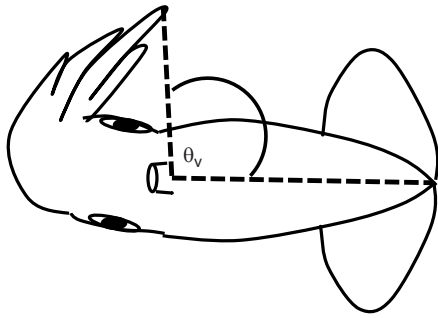
**Fig. 2. *Lolliguncula brevis* turning, demonstrating the wrapping of the arms close to the mantle to decrease the ventral angle between the mantle and arms.** The dashed line illustrates how the ventral angle between the arms and mantle was determined. $\theta_v$, ventral angle between the arms and mantle.



**Fig. 3. The four different postures displayed by *Lolliguncula brevis* and *Sepia bandensis*; only *L. brevis* is pictured for simplicity.** (A) Tail up, arms up. (B) Tail up, arms down. (C) Tail down, arms up. (D) Tail down, arms down. The dashed lines in C demonstrate how the acute angle between the arms and mantle was determined in lateral views. The dashed lines in D demonstrate how the acute angle between the mantle and horizontal was determined in lateral views.
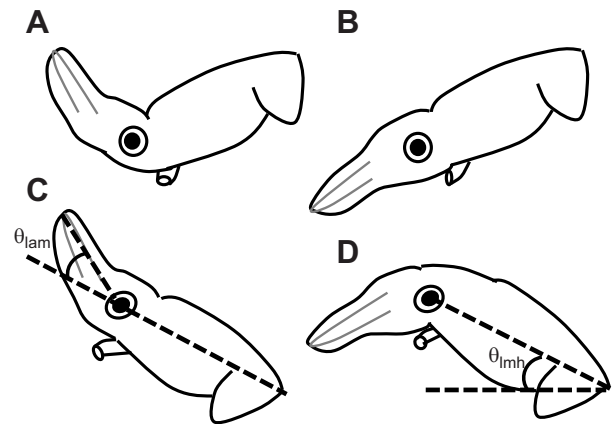
actually have to fall directly on these line segments. Rather, it could lie along a line at a fixed angle $\alpha$ with respect to the tracked body segment, where $\alpha$ and the position of the COR along the line at this angle were selected such that the movement of the COR during the turn was minimized.

The radius ($R$) of the turning path is the radius of curvature of the COR path/trajectory. This was computed from analytical geometry using:

$$\frac{1}{R} = \frac{y''}{\left(1 + (y')^2\right)^{3/2}},$$

where $y' = dy/dx$, $x$ and $y$ are the coordinates of the COR in the ventral view, and the derivatives were evaluated using fourth-order accurate finite difference equations. All reported values, other than absolute values, which derive from individual sequences, are means for individuals. Both the mean radius of the turning path and the minimum radius of the turning path were determined using in-house MATLAB routines. To compare our data with that of previous studies, the minimum and mean radius of the turning path ($R$) was normalized (divided by the total length of the animal) to obtain a length-specific turning radius ($R/L$). $(R/L)_{mean}$ is the average of all COR radii comprising the turning path, divided by the total length of the animal. All of the turning radii values for each sequence were ranked from smallest to largest and the 90th percentile value was considered the minimum $[(R/L)_{min}]$. The 90th percentile value was used to account for frame digitization error, with the 90th percentile being a reasonable cut-off between outliers and more typical values. The absolute minimum $[(R/L)_{a,min}]$ was the lowest 90th percentile minimum from all turn sequences. $\omega_{avg}$ is the mean angular velocity throughout the turn. $\omega_{max}$ is the maximum angular velocity found during the turn, averaged over all turning sequences. $\omega_{a,max}$ is the absolute maximum angular velocity of all turning sequences. Translation was defined as the maximum distance ($D_{max}$; in cm) between the COR at any two instances during the turning sequence, divided by total body length ($D_{max}/L$).

Two different methods were used to calculate turning performance parameters. The first method considered only the mantle segment (DML), using the tail tip point to the funnel base point. The second method considered the total length ($L$) (including the head and arms) of the squid or cuttlefish. In this case, two connected lines were drawn, one from the tail tip point to the funnel base point, and another from the funnel base point to the arm tip point. A nested one-way MANOVA with individual nested within method was performed for each species to determine any

differences between the two methods for each parameter (SPSS, Version 18, IBM, Armonk, NY, USA). There were no significant differences between the two methods for $(R/L)_{min}$, $(R/L)_{mean}$, $\omega_{max}$, $\omega_{avg}$ or $\theta_{total}$ (*L. brevis* MANOVA: $F=0.6$, d.f.=5,40, $P=0.7$; *S. bandensis* MANOVA: $F=2.1$, d.f.=5,98, $P=0.07$). Therefore, only the second method, using $L$, will be presented in all further measurements.

Mantle diameter and angular velocity were smoothed using a fourth-order Butterworth filter and cut-off frequency of 4 Hz. Mantle contraction rate and angular acceleration were calculated from the smoothed data for each sequence by evaluating the derivatives using fourth-order finite difference equations. Jet pulses were identified as periods in which the mantle contraction rate was negative, indicating that mantle diameter was decreasing, and jet pulses shorter than 0.15 s were excluded from analysis. The mantle contraction rate and angular acceleration for jet pulses greater than 0.15 s were analyzed using Pearson correlations.

The tracked points in the lateral view were used to determine: (1) the mantle angle with respect to the horizontal ($\theta_{lmh}$) (Fig. 3D), (2) arm angle with respect to the mantle ($\theta_{lam}$) (Fig. 3C), (3) fin beat amplitude and (4) funnel diameter. These parameters were calculated using MATLAB routines developed in-house. The funnel diameter was not always visible for the entire duration of some turns, thus mantle diameter measured in the ventral view was used to compute jet pulse frequency. Only one fin was consistently visible in lateral views, and therefore fin points in ventral views were used for fin beat analyses in this study. Unfortunately, fin beat frequency was not determined for *S. bandensis* as the fins were too small to resolve consistently in either the lateral or ventral perspectives.

Values that were compared between the two species included $(R/L)_{mean}$, $(R/L)_{min}$, $\omega_{avg}$, $\omega_{max}$, $\theta_{total}$, $\theta_{lmh}$, $\theta_{lam}$, $\theta_{v,min}$, $\Theta_{v,mean}$ and translation. A nested two-way mixed model MANOVA, with individual nested in species, was used to determine whether there was a statistical difference for $(R/L)_{mean}$, $(R/L)_{min}$, $\omega_{avg}$, $\omega_{max}$, $\theta_{total}$, $\theta_{v,min}$, $\theta_{v,mean}$ and translation between the two species (SPSS). A nested two-way mixed model MANOVA with individual nested in posture category was used to determine differences in $\theta_{lmh}$ and $\theta_{lam}$ for *L. brevis* and *S. bandensis*. A log$_{10}$ transformation was used to meet assumptions of normality. The Wilks' lambda test was used for

**Table 1. Kinematic variables for *Lolliguncula brevis* and *Sepia bandensis***

| | $(R/L)_{min}$ | $(R/L)_{mean}$ | $\omega_{max}$ (deg s$^{-1}$) | $\omega_{avg}$ (deg s$^{-1}$) | $\theta_{v,min}$ (deg) | $\theta_{v,mean}$ (deg) | Mantle length percentage (%) |
|---|---|---|---|---|---|---|---|
| *L. brevis* | | | | | | | |
| Minimum | $4.2\times10^{-4}$ | $3.6\times10^{-4}$ | 72.7 | 41.7 | 81.2 | 128.5 | 53.9 |
| Maximum | $1.6\times10^{-2}$ | 0.05 | 725.8 | 390.2 | 171.02 | 176.5 | 66.6 |
| Mean | $3.4\times10^{-3}$ ($5.9\times10^{-4}$) | $8.8\times10^{-3}$ ($3.9\times10^{-3}$) | 268.4 (32.9) | 110.3 (14.6) | 138.9 (5.9) | 161.8 (3.3) | 61.5 (0.8) |
| *S. bandensis* | | | | | | | |
| Minimum | $1.3\times10^{-4}$ | 0.04 | 68.4 | 16.3 | 125.6 | 146.3 | 49.0 |
| Maximum | $2.09\times10^{-2}$ | 0.2 | 485.0 | 109.7 | 172.9 | 177.8 | 64.3 |
| Mean | $1.2\times10^{-3}$ ($4.7\times10^{-4}$) | $9.5\times10^{-2}$ ($3.2\times10^{-2}$) | 160.2 (19.7) | 54.8 (8.4) | 156.4 (2.6) | 167.9 (1.9) | 55.5 (0.8) |

Values in parentheses are standard error of the mean.
$R$, minimum radius of the turning path; $L$, total body length; $(R/L)$, length-specific minimum radius of the turning path [minimum: $(R/L)_{min}$; mean: $(R/L)_{mean}$]; $\omega_{avg}$, average angular velocity of the turn; $\omega_{max}$, maximum instantaneous angular velocity of the turn; $\theta_{v,min}$, minimum ventral angle between the arms and mantle; $\theta_{v,mean}$, mean ventral angle between the arms and mantle; percentage of the mantle from total body length. Minimum and maximum values are absolute minimums and maximums for all turning sequences.

all multivariate analyses (Zar, 2010). To determine whether there was a difference in fin beat frequency for the outboard and inboard fins of *L. brevis*, a paired two-tailed *t*-test was performed (SPSS).

## RESULTS

A total of 36 turns from 14 individuals were analyzed for *L. brevis* and 56 turns from five individuals were analyzed for *S. bandensis*. All subsequent mean values for the results are reported ±s.e.m. Total angular displacement of the turns ranged from 57.5 to 345.1 deg (mean angular displacement=117.2±18.7 deg) for *L. brevis* and from 71.6 to 150.3 deg (mean angular displacement=98.3± 14.0 deg) for *S. bandensis*.

### *Lolliguncula brevis* turning performance

The fin beat frequency was determined for each fin for *L. brevis*, and the fins were characterized as either inboard (fin located in interior of turn) or outboard (fin located at periphery of turn) in relation to the turning direction. The outboard fin beat frequency (mean=3.5±0.2 beats s$^{-1}$) was significantly higher than the inboard fin beat frequency (mean=2.9±0.2 beats s$^{-1}$) during turning maneuvers (paired *t*-test: *t*=2.8, d.f.=13, *P*<0.05). The few turns that involved similar fin beat frequencies on each side, or that had a higher inboard frequency than outboard frequency, often were not synchronized, or there was a phase shift between the inboard and outboard sides.

$(R/L)_{min}$ was $3.4\times10^{-3}$±$5.9\times10^{-4}$, with $(R/L)_{a,min}$=$4.2\times10^{-4}$ and $(R/L)_{mean}$=$8.8\times10^{-3}$±$3.9\times10^{-3}$ (Table 1). The range in $(R/L)_{mean}$ values was 0.0004 to 0.05. $\omega_{avg}$ was 110.3±14.6 deg s$^{-1}$, $\omega_{max}$ was 268.4±32.9 deg s$^{-1}$ and $\omega_{a,max}$ was 725.8 deg s$^{-1}$ (Table 1). A trend

in increased $\omega_{max}$ with increased $(R/L)_{min}$ is illustrated in Fig. 4, though the correlation was not significant at *P*=0.05. As $\omega_{max}$ increased, the $\theta_{v,min}$ decreased (Pearson correlation: *r*=0.7, d.f.=13, *P*=0.005), and as $\omega_{avg}$ increased, the $\theta_{v,mean}$ decreased (Pearson correlation: *r*=0.7, d.f.=13, *P*=0.01) (Fig. 5).

The 36 turns for *L. brevis* were divided into four different orientations: (1) tail and arms up, (2) tail up and arms down, (3) tail down and arms up, and (4) tail and arms down (Fig. 3). The most commonly observed orientation was tail and arms up (orientation 1, 19 turns). Tail up arms down (orientation 2) and tail down arms up (orientation 3) were observed in six and eight turns, respectively, and lastly, tail and arms down (orientation 4, three turns) was the least common. There were no significant differences among any turning parameters or body angles among the different orientations even if turns were pooled into tail up versus tail down and arms up versus arms down orientations.

Mantle contraction rate generally correlated with angular acceleration, indicating a relationship between the jet pulse and angular velocity, with some sequences correlating very strongly (Pearson correlation: *r*>0.6, *P*<0.005). Specifically, angular acceleration increased with increased mantle contraction rate (Fig. 6). Generally, the highest angular velocity occurred shortly after mid mantle contraction (Fig. 7). During turns, multiple fin beats were employed during each mantle contraction. The fin beats on the outboard and inboard sides were usually synchronized for the majority of the turn, and often became asynchronous towards the middle to end of the turn (Fig. 8). The difference in average beat frequency was driven by one or two main periods of fin asymmetry during a single turn sequence. Asymmetric fin motions often
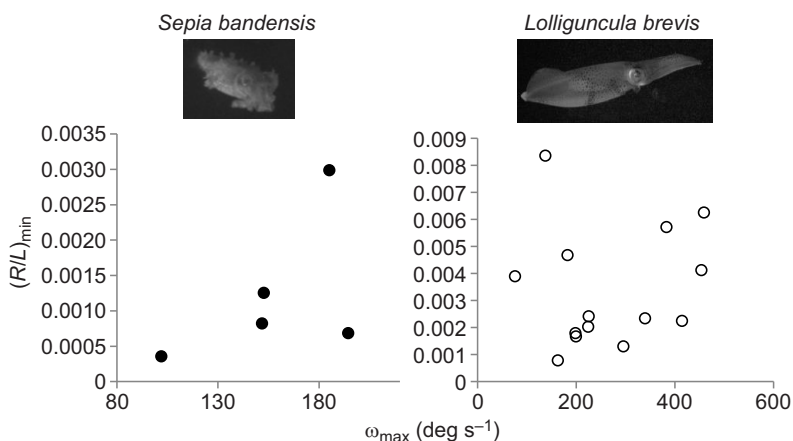


**Fig. 4. Relationship between the length-specific minimum radius of the turn [$(R/L)_{min}$] and maximum angular velocity ($\omega_{max}$) for *Sepia bandensis* (left, *N*=5) and *Lolliguncula brevis* (right, *N*=14).** Only the *S. bandensis* relationship is significant (Pearson correlation: *r*=0.9, d.f.=4, *P*=0.04).
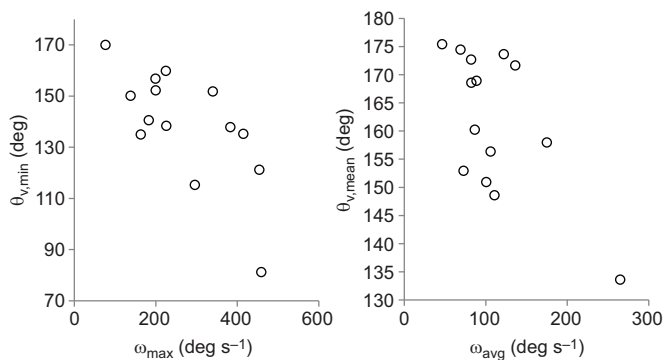
**Fig. 5. Relationship between the ventral angle between the arms and mantle and angular velocity for *Lolliguncula brevis*.** (A) Relationship between minimum ventral arm/mantle angle ($\theta_{v,min}$) and maximum angular velocity ($\omega_{max}$; N=14). The relationship is significant (Pearson correlation: r=0.7, d.f.=13, P=0.005). (B) Relationship between mean ventral arm/mantle angle ($\theta_{v,mean}$) and mean angular velocity ($\omega_{avg}$; N=14). The relationship is significant (Pearson correlation: r=0.7, d.f.=13, P=0.01).

occurred at the same time as the more dominant jet, making it difficult to evaluate clear fin-related impacts on angular velocity. Though fin action generally did not influence angular velocity as substantially as the jet, some forceful fin beats did contribute to obvious spikes in angular velocity, which were superimposed onto the dominant jet-driven angular velocity patterns.

### *Sepia bandensis* turning performance

$(R/L)_{min}$ was $1.2 \times 10^{-3} \pm 4.7 \times 10^{-4}$, with $(R/L)_{a,min}=1.3 \times 10^{-4}$ and $(R/L)_{mean}=9.5 \times 10^{-2} \pm 3.2 \times 10^{-2}$ (Table 1). The range of $(R/L)_{mean}$ values was 0.04 to 0.2. $\omega_{avg}$ was $54.8 \pm 8.4$ deg s$^{-1}$, mean $\omega_{max}$ was $160.2 \pm 19.7$ deg s$^{-1}$ (Table 1) and $\omega_{a,max}$ was 485.0 deg s$^{-1}$. As $(R/L)_{min}$ increased, $\omega_{max}$ also increased (Pearson correlation: r=0.9, d.f.=4, P=0.04; Fig. 4). There was no correlation of $(R/L)$ or $\omega$ with $\theta_v$.

As was the case for squid, the 56 turns for *S. bandensis* could be classified according to four different orientations: (1) tail and arms up, (2) tail up and arms down, (3) tail and arms down, and (4) tail down and arms up. The most commonly observed orientation was tail up arms down (orientation 2, 20 turns). Tail and arms down (orientation 3), tail and arms up (orientation 1) and tail down and
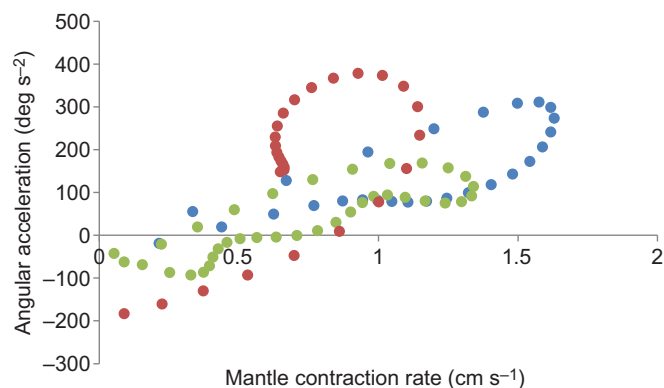


**Fig. 6. Angular acceleration plotted against mantle contraction rate for three separate jet pulses.** The jet pulses are from three different turning sequences. Positive values for angular acceleration are indicative of increasing speed while negative values for angular acceleration are indicative of decreasing speed. The Pearson correlation coefficients for these particular pulses are r=0.8 (blue circles), 0.7 (red circles) and 0.8 (green circles) with all P-values <0.001.

arms up (orientation 4) were observed in 15, 11 and 10 of the turns, respectively. There were no significant differences for turning parameters or body angles among the four orientations even if turns were pooled into either tail up versus tail down or arms up versus arms down groupings. The only significant difference found for body orientation was that the arm angle relative to the mantle was significantly steeper for the arms down orientation (mean=$21.4 \pm 3.8$ deg) than the arms up orientation (mean=$10.2 \pm 1.8$ deg; MANOVA: F=4.9, d.f.=1,19, P=0.04).

### Species comparison

*Sepia bandensis* $(R/L)_{min}$ (mean=$1.2 \times 10^{-3} \pm 4.710^{-4}$) was significantly lower than that for *L. brevis* (mean=$3.4 \times 10^{-3} \pm 5.9 \times 10^{-4}$; MANOVA: F=6.6, d.f.=8,66, P=0.01). However, $(R/L)_{mean}$ was not significantly different for *L. brevis* (mean=$8.8 \times 10^{-3} \pm 3.9 \times 10^{-3}$) and *S. bandensis* (mean=$9.5 \times 10^{-2} \pm 3.2 \times 10^{-2}$; MANOVA: F=3.0, d.f.=8,66, P>0.05). $\omega_{max}$ was significantly greater for *L. brevis* (mean=$268.4 \pm 32.9$ deg s$^{-1}$) than for *S. bandensis* (mean=$160.2 \pm 19.7$ deg s$^{-1}$; MANOVA: F=8.008, d.f.=8,66, P=0.006), and $\omega_{avg}$ was also significantly greater for *L. brevis* (mean=$110.3 \pm 14.6$ deg s$^{-1}$) than for *S. bandensis* (mean=$54.8 \pm 8.4$ deg s$^{-1}$; MANOVA: F=22.5, d.f.=8,66, P<0.001). There was no significant difference in $\theta_{total}$ between the two species (MANOVA: F=0.4, d.f.=8,66, P>0.05). The $\theta_{v,min}$ was significantly less for *L. brevis* (mean=$138.9 \pm 5.9$ deg) than for *S. bandensis* (mean=$156.4 \pm 2.6$ deg; MANOVA: F=6.8, d.f.=8,66, P=0.01) during turns. The $\theta_{v,mean}$ was also significantly lower for *L. brevis* (mean=$161.8 \pm 3.3$ deg) than for *S. bandensis* (mean=$167.9 \pm 1.9$ deg; MANOVA: F=5.2, d.f.=8,66, P=0.03). There was no significant difference in translation between *L. brevis* turning maneuvers (mean=$0.2 \pm 0.02$) and *S. bandensis* turning maneuvers (mean=$0.1 \pm 0.01$; MANOVA: F=1.2, d.f.=8,66, P>0.05), though *S. bandensis* did exhibit a trend in more tightly grouped COR values (Fig. 9). The only other body orientation parameter that differed between the species was the angle of the arms with the mantle, which was significantly steeper for *L. brevis* in the arms down orientation (mean=$18.3 \pm 5.8$ deg) than *S. bandensis* in the arms up orientation (mean=$10.2 \pm 1.8$ deg; MANOVA: F=1.8, d.f.=3,28.7, P=0.02).

### DISCUSSION

Squid and cuttlefish represent a unique group of aquatic animals, relying on two dissimilar propulsors ( jet and fins) that are powered by obliquely striated muscles in a hydrostatic arrangement. Both squid and cuttlefish swim using a combination of paired fin movements and a pulsed jet that can be vectored in any direction within a hemisphere below the body. Using this dual-mode system, squids and cuttlefishes are capable of a wide repertoire of unsteady turning motions. This study represents the first quantitative study of turning performance in any cephalopod. Both species of cephalopods considered in this study were found to be highly maneuverable with absolute length-specific minimum radii of their turns approaching zero, i.e. 0.00042 for *L. brevis* and 0.00013 for *S. bandensis*. In addition, *L. brevis* had greater agility ($\omega_{a,max}$=726 deg s$^{-1}$) than *S. bandensis* ($\omega_{a,max}$=485 deg s$^{-1}$), though *S. bandensis* exhibited the capacity for more controlled turns with many examples of tight grouping of the COR. During turns for *L. brevis*, angular velocity was driven, to a large extent, by the pulsed jet with the fins playing a more subordinate role.

The level of flexibility in aquatic swimmers can impact turning performance. There is some evidence that suggests this flexibility and increased turning performance results in decreased stability, or that the increase in turning performance is a consequence of
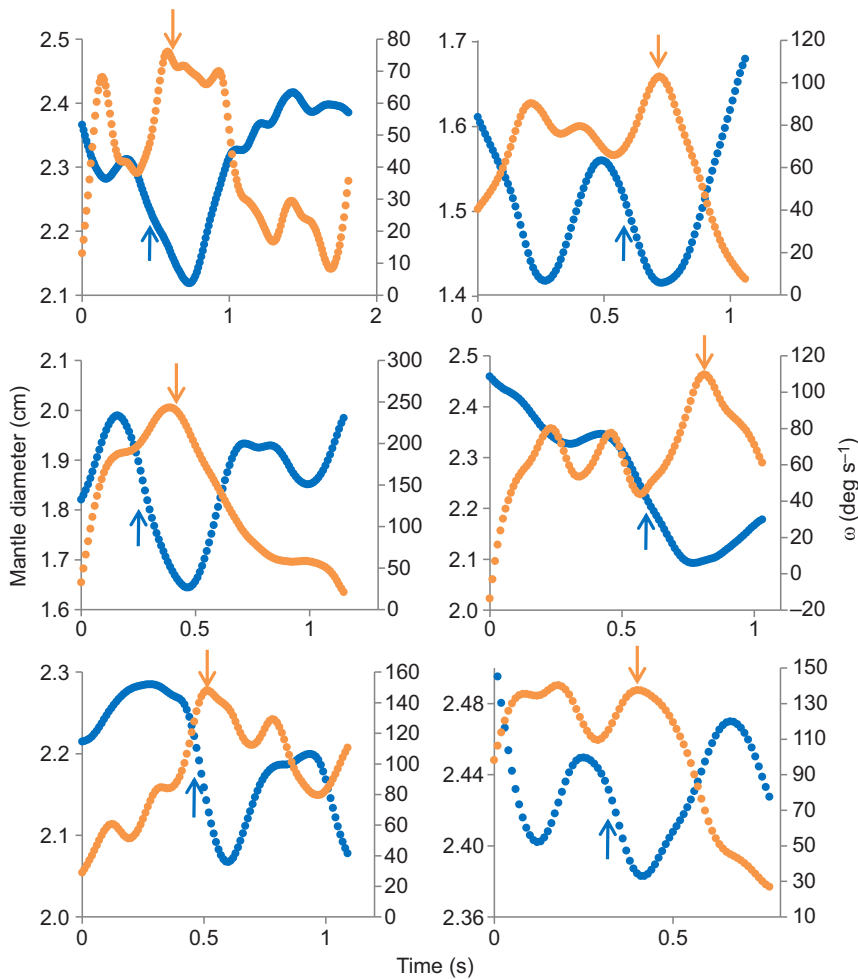
**Fig. 7. Mantle diameter (blue circles) and angular velocity (orange circles) for six different *Lolliguncula brevis* turning sequences.** Mantle diameter and angular velocity data were smoothed using a fourth-order Butterworth filter and cut-off frequency of 4 Hz. Decreasing mantle diameter is indicative of contraction resulting in a pulsed jet. Peak angular velocity (orange arrows) generally follows shortly after the mid-point of the mantle contraction (blue arrows). Angular velocity appears to be driven primarily by the jet pulse with angular velocity beginning to increase shortly after the mantle begins contracting.

decreased stability (Fish et al., 2003). Squid do have some characteristics of a stable body; however, the flexibility of the propulsors (jet and fins) combined with flexible control surfaces (fins and arms) allow squid to easily override static stability when necessary to achieve high maneuverability. Squid employ propulsors (fins) and control surfaces (fins and arms) that are located distant from their center of mass. Having these propulsors and control surfaces so far from the center of mass allows these animals to produce corrective moments that are capable of enhancing both stability and maneuverability.

Several studies investigating turning performance of rigid-bodied aquatic taxa have demonstrated that a rigid body does not necessarily limit turning performance due to the contribution of propulsors and control surfaces (Fish and Nicastro, 2003; Parson et al., 2011; Rivera et al., 2006; Walker, 2000). Squid and cuttlefish have a chitinous pen and cuttlebone, respectively, that constrict bending and length changes in the mantle, though their arms are flexible. Thus cephalopods do not fit neatly into the flexible, stiff and rigid-bodied categories described earlier. Nonetheless, comparisons between cephalopods and other nekton that do fit within these categories are constructive. Previously, the rigid-bodied spotted boxfish, *Ostracion meleagris*, was considered the most maneuverable aquatic animal, with a mean length-specific minimum radius of the turn of 0.0325 and an absolute minimum of 0.0005 (Walker, 2000). These values were based on one individual performing 12 turning sequences. Comparable values for *S. bandensis* and *L. brevis* in this study are $1.2 \times 10^{-3}$ and $3.4 \times 10^{-3}$,

respectively, for $(R/L)_{min}$, which are orders of magnitude below the values for boxfish, and $1.3 \times 10^{-4}$ and $4.2 \times 10^{-4}$, respectively, for $(R/L)_{a,min}$, which are also lower than those of boxfish. The values given here for $(R/L)_{min}$ are conservative, as the 90th percentile $R/L$ value was used for each turning sequence, instead of the absolute minimum for each sequence. This ensured that any extreme values that could be due to digitization error were accounted for. Taking minimum values from the 90th percentile of each turning sequence, averaging these minimum values per individual and then taking an average of all the individual minima to calculate $(R/L)_{min}$ gives a much more representative and conservative estimate of maximum maneuvering capability.

The mean, $(R/L)_{mean}$, was also low for both cephalopods, with values of $9.5 \times 10^{-2}$ for *S. bandensis* and $8.8 \times 10^{-3}$ for *L. brevis* (Table 1). Given the lower mean $(R/L)_{min}$ values for *S. bandensis*, and their capacity for low translation (see Fig. 9), we expected $(R/L)_{mean}$ to be lower for *S. bandensis*. However, this was not observed, with $(R/L)_{mean}$ values being lower for *L. brevis*. This finding likely reflects behavioral variability. Although *S. bandensis* is capable of achieving a very low $(R/L)_{min}$, it does not always turn at this performance extreme. Instead, it uses a wide range of turning behaviors, which is reflected in the observed greater $(R/L)_{mean}$ range for *S. bandensis* relative to *L. brevis*, and similar values for length-specific translation. When $(R/L)_{mean}$ is considered, *L. brevis* still ranks as the most maneuverable aquatic animal measured to date. Though *S. bandensis* did demonstrate the capability of tighter turns, as seen in the $(R/L)_{min}$, *S. bandensis* is closer to pike, *Esox lucius*
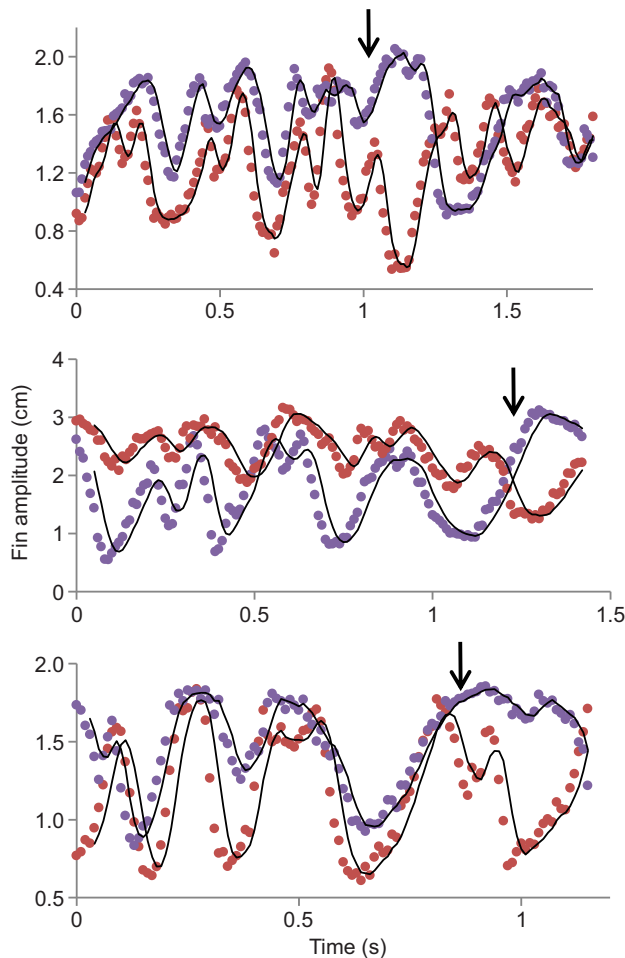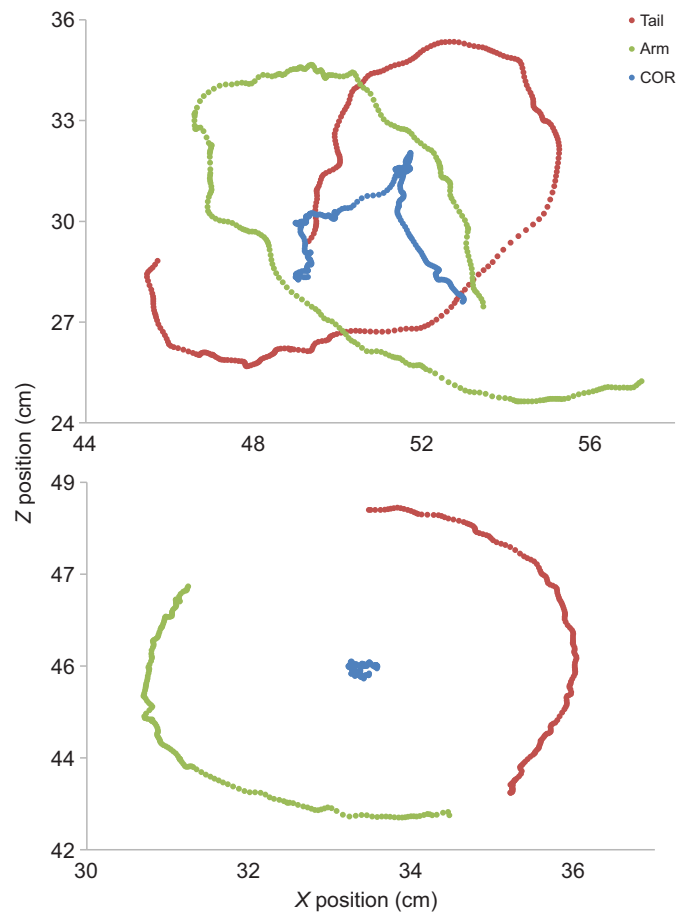
**Fig. 8. Fin amplitude plotted for three different *Lolliguncula brevis* turning sequences, with the outboard fin (red circles) and the inboard fin (purple circles).** Generally, the fin beats are synchronized through the majority of the turn, with one or two main periods of asymmetry occurring late in the turn (black arrows).



**Fig. 9. Turning path trajectories from one turning sequence for *Lolliguncula brevis* (top) and *Sepia bandensis* (bottom).** The blue circles are the center of rotation (COR) path throughout the turn, red circles are the tail tip point and the green circles are the arm tip point. The data were smoothed using a cross-validation criterion filter (see Materials and methods).

(Domenici and Blake, 1997), and the dolphinfish, *Coryphaena hippurus* (Webb and Keyes, 1981), in terms of maneuverability when the $(R/L)_{mean}$ is considered.

As $\omega_{max}$ increased, $(R/L)_{min}$ also increased for *S. bandensis*, with a similar trend observed for *L. brevis*. This finding was expected and indicative of faster turns also being wider turns. As turns become faster and inertia increases, it becomes more difficult to control the tightness of the turn, resulting in higher length-specific turning radii. Turning speed, measured as angular velocity ($\omega$), was also quite high for *L. brevis* and *S. bandensis*. The observed values of $\omega_{a,max}$=485.0 deg s$^{-1}$ (mean $\omega_{max}$=160.2 deg s$^{-1}$) for *S. bandensis* and $\omega_{a,max}$=725.8 deg s$^{-1}$ (mean $\omega_{max}$=268.4 deg s$^{-1}$) for *L. brevis* are higher than peak turning speeds for spotted boxfish ($\omega_{a,max}$=218 deg s$^{-1}$) and, for *L. brevis*, higher than painted turtles (501.8 deg s$^{-1}$) (Rivera et al., 2006; Walker, 2000). Indeed, the values for *S. bandensis* are comparable to those reported for yellowfin tuna ($\omega_{a,max}$=426 deg s$^{-1}$) (Blake et al., 1995) and painted turtles, and the values for *L. brevis* exceed those of more flexible-bodied taxa, such as sea lions ($\omega_{a,max}$=690 deg s$^{-1}$) (Fish et al., 2003).

Consideration of size effects on agility is important, as smaller animals generally achieve greater levels of agility than larger animals (?Alexander, 1967</TRCOL). When agility measures for

*L. brevis* and *S. bandensis* are compared as a function of size with those for all aquatic taxa measured to date, they fall just below a line separating flexible-bodied and rigid-bodied taxa (see fig. 7 in Fish and Nicastro, 2003). *Lolliguncula brevis* has greater agility (725.8 deg s$^{-1}$) than similar sized rigid-bodied aquatic taxa, such as the spotted boxfish (218 deg s$^{-1}$) and painted turtle (501.8 deg s$^{-1}$); *S. bandensis* (485.0 deg s$^{-1}$) has greater agility than boxfish but similar agility to painted turtles (Rivera et al., 2006; Walker, 2000). Flexible-bodied reef fish of similar size, however, have greater agility than *L. brevis* and *S. bandensis* (bluehead wrasse: 3625 deg s$^{-1}$, ocean surgeonfish: 7300 deg s$^{-1}$, beaugregory damselfish: 4924 deg s$^{-1}$ and foureye butterflyfish: 4730 deg s$^{-1}$) (Gerstner, 1999). *Lolliguncula brevis* displays greater agility than some larger flexible bodied marine mammals (sea lion: 690 deg s$^{-1}$) and stiff-bodied fish (yellowfin tuna: 426 deg s$^{-1}$), though larger animals must overcome a greater amount of drag while turning than smaller animals (Blake et al., 1995; Fish et al., 2003). These findings reflect the hybrid body architecture of squid and cuttlefish, which consists of both rigid and flexible components.

Flexible-bodied animals can bend their body axis to minimize the length of the body creating drag during the turn. Rigid-bodied animals cannot bend in this way, so the entire rigid portion of the body will resist rotation, often leading to lower turning speeds. The dorsal region of the *L. brevis* mantle is inflexible as a result of the chitinous pen, but it can compensate for this inflexible component

by wrapping its arms close to the mantle. Despite having a more restrictive cuttlebone in its mantle and a relatively longer head and arms than *L. brevis* (44.6±0.8% total body length versus 38.5±0.8% in *L. brevis*), *S. bandensis* did not display this arm wrapping behavior as prominently as *L. brevis* (based on higher ventral arm/mantle angles). Thus, greater arm drag could help explain the lower observed $\omega_{max}$ for *S. bandensis*.

The arm positioning relative to the body impacted turning performance for *L. brevis*. As the mean and minimum angle between the arms and mantle decreased in *L. brevis*, $\omega_{mean}$ and $\omega_{max}$ increased, respectively. This is expected, as bending any part of the body axis reduces the body's moment of inertia about the dorsoventral rotational axis, resulting in lower inertial resistance to rotation and lower hydrodynamic rotational resistance (Walker, 2000). Therefore, *L. brevis* wraps its arms towards the mantle to achieve faster turns. Though *S. bandensis* was also capable of wrapping its arms to the mantle, it generally did so at higher minimum and mean ventral angles than *L. brevis*. Moreover, the ventral angle between the arms and mantle was not correlated with angular velocity or the minimum radius for *S. bandensis*. These differences may derive from how the turns were performed. Turns for *S. bandensis* were often prompted by moving a prey item around the experimental chamber, which was not necessary for *L. brevis*. Because cephalopods orient arms-first towards prey items, *S. bandensis* may have been tracking the prey with its arms rather than bending them close to the body to increase angular velocity.

The interplay between the jet and fins plays an important role in turning performance in cephalopods. Although fin motions were not quantified for *S. bandensis* because of the small size and translucency of the fins, they were clearly active during turns and likely aided turning, as was the case for *L. brevis*. In *L. brevis*, the outboard fin on the far side of the turn beat significantly faster than the inboard fin on the near side of the turn, and the turning sequence with the highest $\omega_{max}$ corresponded with the greatest difference in fin beats on the far and near side of the turn. However, there were also some turning sequences where angular velocity was high and/or $(R/L)_{min}$ was low, without a large difference in fin beat frequency between the fins. In these sequences, the timing of the fin beats seemingly was more important than mean frequency and/or the jet played a larger role in these turns. To help determine the role the jet played in turns, the mantle contraction, angular velocity and fin amplitudes were tracked throughout turning sequences. In general, the highest angular velocity throughout turning sequences closely followed strong mantle contractions and mantle contraction rate correlated with angular acceleration, suggesting that the jet contributes more to agility, i.e. the speed of the turn, than the fins. The fins appeared to be synchronized throughout most of the turn but became asynchronous for several fin strokes midway through the turn or towards the end of the turn. During these instances, the outboard and inboard fin exhibited different flapping frequencies. Though this asymmetry may have contributed to small increases in angular velocity, the impact of the fins on turning velocity were often masked by the jet and difficult to fully evaluate. In some sequences, however, forceful fin flaps did produce angular velocity spikes superimposed on the larger jet-driven velocity patterns, indicating that fins can indeed impact angular velocity patterns, albeit to a lesser extent than the jet. Although not examined specifically in this paper, the fins are likely important for controlling the stability of the turn, and in minimizing the length-specific radius of the turn. Although the same four postures were observed in both *L. brevis* and *S. bandensis*, different postures were more prevalent in each species. These postures, however, do not appear to influence

turning performance to a significant extent based on the results of this study.

*Sepia bandensis* had many turns where the COR was very tightly grouped, while *L. brevis* had more turning sequences where the COR path exhibited long arms before and after an area of tight grouping. When translation during the turn was normalized using total body length, no difference was observed between *S. bandensis* and *L. brevis*, but it would appear that *S. bandensis* is at least capable of turns with very little translation because the long arms of the COR turning path were not a prominent feature of turning sequences. *Sepia bandensis* possesses an internal cuttlebone that allows it to maintain neutral buoyancy, which is not achievable in *L. brevis*. With neutral buoyancy, cuttlefish do not need to constantly direct flows downward for lift production, either through jetting or fin movements. In *L. brevis*, downward jet-and/or fin-derived forces are required at all times for lift production, even when thrust is not required, and this constant fin/jet vectoring likely leads to greater drift during turns. Having fins that extend along the entire mantle, like *S. bandensis*, also provides more longitudinal control surfaces that can potentially limit translational movements. *Sepia bandensis* has fins with a longer chord length but smaller span than *L. brevis*, which may facilitate finer force control.

## Concluding thoughts

*Lolliguncula brevis* and *S. bandensis* are highly maneuverable, with *R/L* values that are the lowest reported to date for any aquatic animal, and are more agile than similar-sized rigid-bodied nekton and larger flexible-bodied swimmers. However, they have lower agility than flexible fish of similar size. These comparisons illustrate that the unique hybrid body architecture of squid and cuttlefish does not necessarily result in a trade-off between maneuverability and agility, as seen in some rigid-bodied taxa (Fish and Nicastro, 2003; Walker, 2000). Although moving the flexible elements of the body, such as the arms, does appear to impact turning performance to some degree, the fins and jet are extremely active during turns and are the primary drivers of turning performance. The shallow coastal sandy and reef habitats that these cephalopods reside in require a high level of turning performance. Mobile inhabitants of these environments must be able to effectively navigate in and around complex structures, and hide in small crevices and openings to avoid predators, and thus high maneuverability is important. The tail-first orientation is preferred over the arms-first orientation for steady swimming (Bartol et al., 2001a), but squid and cuttlefish always orient arms-first to attack prey (Foyle and O'dor, 1988; Kier and Van Leeuwen, 1997; Messenger, 1968), making arms-first turning integral for their survival. Not surprisingly, squid and cuttlefish are both effective at turning in the arms-first mode. Given that squid and cuttlefish are also effective predators as well as common prey targets, it is important for them to exhibit moderate levels of agility, as turning is essential for both capturing prey and escaping from predators. Thus evolutionary pressures may have contributed to increased maneuverability and agility in terms of extreme turning limits, control of turns and overall turning flexibility, all of which are reflected in the performance findings of this study.

**Competing interests**
The authors declare no competing or financial interests.

**References**

**Alexander, R. M.** (1967). *Functional Design in Fishes*. London: Hutchinson University Library.

**Anderson, E. J. and DeMont, M. E.** (2000). The mechanics of locomotion in the squid *Loligo pealei*: locomotory function and unsteady hydrodynamics of the jet and intramantle pressure. *J. Exp. Biol.* **203**, 2851-2863.

**Anderson, E. J. and Grosenbaugh, M. A.** (2005). Jet flow in steadily swimming adult squid. *J. Exp. Biol.* **208**, 1125-1146.

**Bartol, I. K., Patterson, M. P. and Mann, R.** (2001a). Swimming mechanics and behavior of the shallow-water brief squid *Lolliguncula brevis*. *J. Exp. Biol.* **204**, 3655-3682.

**Bartol, I. K., Mann, R. and Patterson, M. R.** (2001b). Aerobic respiratory costs of swimming in the negatively buoyant brief squid *Lolliguncula brevis*. *J. Exp. Biol.* **204**, 3639-3653.

**Bartol, I. K., Krueger, P. S., Thompson, J. T. and Stewart, W. J.** (2008). Swimming dynamics and propulsive efficiency of squids throughout ontogeny. *Int. Comp. Biol.* **48**, 720-733.

**Bartol, I. K., Krueger, P. S., Stewart, W. J. and Thompson, J. T.** (2009a). Hydrodynamics of pulsed jetting in juvenile and adult brief squid *Lolliguncula brevis*: evidence of multiple jet 'modes' and their implications for propulsive efficiency. *J. Exp. Biol.* **212**, 1889-1903.

**Bartol, I. K., Krueger, P. S., Stewart, W. J. and Thompson, J. T.** (2009b). Pulsed jet dynamics of squid hatchlings at intermediate Reynolds numbers. *J. Exp. Biol.* **212**, 1506-1518.

**Bartol, I. K., Krueger, P. S., Jastrebsky, R. A., Williams, S. and Thompson, J. T.** (2016). Volumetric flow imaging reveals the importance of vortex ring formation in squid swimming tail-first and arms-first. *J. Exp. Biol.* **219**, 392-403.

**Blake, R. W.** (1977). On ostraciiform locomotion. *J. Mar. Biol. Assoc. UK* **57**, 1047-1055.

**Blake, R. W., Chatters, L. M. and Domenici, P.** (1995). Turning radius of yellowfin tuna (*Thunnus albacares*) in unsteady swimming manoeuvres. *J. Fish Biol.* **46**, 536-538.

**Boyle, P. and Rodhouse, P.** (2005). *Cephalopods: Ecology and Fisheries*. Oxford, UK: Blackwell Science, Ltd.

**Denton, E. J. and Gilpin-Brown, J. B.** (1961). The buoyancy of the cuttlefish, *Sepia officinalis* (L.). *J. Mar. Biol. Assoc. UK* **41**, 319-342.

**Domenici, P. and Blake, R. W.** (1991). The kinematics and performance of the escape response in the angelfish (*Pterophyllum eimekei*). *J. Exp. Biol.* **156**, 187-205.

**Domenici, P. and Blake, R. W.** (1997). The kinematics and performance of fish fast-start swimming. *J. Exp. Biol.* **200**, 1165-1178.

**Domenici, P., Standen, E. M. and Levine, R. P.** (2004). Escape manoeuvres in the spiny dogfish (*Squalus acanthias*). *J. Exp. Biol.* **207**, 2339-2349.

**Drucker, E. G. and Lauder, G. V.** (1999). Locomotor forces on a swimming fish: three-dimensional vortex wake dynamics quantified using digital particle image velocimetry. *J. Exp. Biol.* **202**, 2393-2412.

**Drucker, E. G. and Lauder, G. V.** (2000). Hydrodynamic analysis of fish swimming speed: wake structure and locomotor force in slow and fast labriform simmers. *J. Exp. Biol.* **203**, 2379-2393.

**Fish, F. E.** (1993). Power output and propulsive efficiency of swimming bottlenose dolphins (*Tursiops truncatus*). *J. Exp. Biol.* **185**, 179-193.

**Fish, F. E.** (1994). Influence of hydrodynamic-design and propulsive mode on mammalian swimming energetics. *Aust. J. Zool.* **42**, 79-101.

**Fish, F. E.** (2002). Balancing requirements for stability and maneuverability in cetaceans. *Integr. Comp. Biol.* **42**, 85-93.

**Fish, F. E. and Nicastro, A. J.** (2003). Aquatic turning performance by the whirligig beetle: constraints on maneuverability by a rigid biological system. *J. Exp. Biol.* **206**, 1649-1656.

**Fish, F. E., Hurley, J. and Costa, D. P.** (2003). Maneuverability by the sea lion Zalophus californianus: turning performance of an unstable body design. *J. Exp. Biol.* **206**, 667-674.

**Fish, F. E., Howle, L. E. and Murray, M. M.** (2008). Hydrodynamic flow control in marine mammals. *Integr. Comp. Biol.* **48**, 788-800.

**Foyle, T. P. and O'Dor, R. K.** (1988). Predatory strategies of squid (*Illex illecebrosus*) attacking small and large fish. *Mar. Behav. Phys.* **13**, 155-168.

**Gerstner, C. L.** (1999). Maneuverability of four species of coral-reef fish that differ in body and pectoral-fin morphology. *Can. J. Zool.* **77**, 1102-1110.

**Gray, J.** (1933). Directional control of fish movement. *Proc. R. Soc. B Biol. Sci.* **113**, 115-125.

**Harper, D. G. and Blake, R. W.** (1990). Fast-start performance of rainbow trout *Salmo gairdneri* and northern pike *Esox lucius*. *J. Exp. Biol.* **150**, 321-342.

**Hedrick, T. L.** (2008). Software techniques for two- and three-dimensional kinematic measurements of biological and biomimetic systems. *Bioinspir. Biomim.* **3**, 6.

**Hoar, J. A., Sim, E., Webber, D. M. and O'Dor, R. K.** (1994). The role of fins in the competition between squid and fish. In *Mechanics and Physiology of Animal Swimming* (ed. L. Maddock, Q. Bone and J. M. V. Rayner), pp. 27-43. Cambridge: Cambridge University Press.

**Kasapi, M. A., Domenici, P., Blake, R. W. and Harper, D.** (1993). The kinematics and performance of escape responses of the knifefish *Xenomystus nigri*. *Can. J. Zool.* **71**, 189-195.

**Kier, W. M. and Van Leeuwen, J.** (1997). A kinematic analysis of tentacle extension in the squid *Loligo pealei*. *J. Exp. Biol.* **200**, 41-53.

**Kier, W. M., Smith, K. K. and Miyan, J. A.** (1989). Electromyography of the fin musculature of cuttlefish, *Sepia officinalis*. *J. Exp. Biol.* **143**, 17-31.

**Liao, J. C., Beal, D. N., Lauder, G. V. and Triantafyllou, M. S.** (2003). Fish exploiting vortices decrease muscle activity. *Science* **302**, 1566-1569.

**Maia, A. and Wilga, C. D.** (2013). Function of dorsal fins in bamboo shark during steady swimming. *Zoology* **116**, 224-231.

**Maresh, J. L., Fish, F. E., Nowacek, D. P., Nowacek, S. M. and Wells, R. S.** (2004). High performance turning capabilities during foraging by bottlenose dolphins (*Tursiops truncatus*). *Mar. Mamm. Sci.* **20**, 498-509.

**Messenger, J. B.** (1968). The visual attack of the cuttlefish, *Sepia officinalis*. *Anim. Behav.* **16**, 342-357.

**Norberg, U. and Rayner, J. M. V.** (1987). Ecological morphology and flight in bats (Mammalia; Chiroptera): wing adaptations, flight performance, foraging strategy and echolocation. *Philos. Trans. R. Soc. B Biol. Sci.* **316**, 335-427.

**O'Dor, R. K.** (1988). The forces acting on swimming squid. *J. Exp. Biol.* **137**, 421-442.

**Parson, J. M., Fish, F. E. and Nicastro, A. J.** (2011). Turning performance of batoids: limitations of a rigid body. *J. Exp. Mar. Biol. Ecol.* **402**, 12-18.

**Rivera, G., Rivera, A. R. V., Dougherty, E. E. and Blob, R. W.** (2006). Aquatic turning performance of painted turtles (*Chrysemys picta*) and functional consequences of a rigid body design. *J. Exp. Biol.* **209**, 4203-4213.

**Stewart, W. J., Bartol, I. K. and Krueger, P. S.** (2010). Hydrodynamic fin function of brief squid, *Lolliguncula brevis*. *J. Exp. Biol.* **213**, 2009-2024.

**Thompson, J. T. and Kier, W. M.** (2001). Ontogenetic changes in mantle kinematics during escape-jet locomotion in the oval squid, *Sepioteuthis lessoniana Lesson, 1830. Biol. Bull.* **201**, 154-166.

**Walker, J. A.** (1998). Estimating velocities and accelerations of animal locomotion: a simulation experiment comparing numerical differentiation algorithms. *J. Exp. Biol.* **201**, 981-995.

**Walker, J. A.** (2000). Does a rigid body limit maneuverability? *J. Exp. Biol.* **203**, 3391-3396.

**Webb, P. W.** (1975). Hydrodynamics and energetics of fish propulsion. *Bull. Fish Res. Board Can.* **190**, 1-159.

**Webb, P. W.** (1978). Fast-start performance and body form in seven species of teleost fish. *J. Exp. Biol.* **74**, 211-226.

**Webb, P. W.** (1983). Speed, acceleration and maneuverability in seven species of teleost fish. *J. Exp. Biol.* **102**, 115-122.

**Webb, P. W.** (1984). Form and function in fish swimming. *Sci. Am.* **251**, 72-82.

**Webb, P. W.** (1994). The biology of fish swimming. In *Mechanics and Physiology of Animal Swimming* (ed. L. Maddock, Q. Bone and J. M. V. Rayner), pp 45-62. Cambridge: Cambridge University Press.

**Webb, P. W. and Keyes, R. S.** (1981). Division of labor between median fins in swimming dolphin (Pisces: Coryphaenidae). *Copeia* **1981**, 910-904.

**Weihs, D.** (1972). A hydrodynamical analysis of fish turning manoeuvres. *Proc. R. Soc. B Biol. Sci.* **182**, 59-72.

**Weihs, D.** (1993). Stability of aquatic animal locomotion. *In Contemporary Mathematics: Fluid Dynamics in Biology* (ed. Cheer, A. Y. and van Dam, C. P.), pp. 443-462. Seattle, WA: American Mathematical Society.

**Wells, M. J. and O'Dor, R. K.** (1991). Jet propulsion and the evolution of cephalopods. *Bull. Mar. Sci.* **49**, 419-432.

**Wilga, C. D. and Lauder, G. V.** (2000). Three-dimensional kinematics and wake structure of the pectoral fins during locomotion in the leopard shark, *Triakis semifasciata*. *J. Exp. Biol.* **203**, 2261-2278.

**Zar, J. H.** (2010). *Biostatistical Analysis*, 5th edn. Pearson. Upper Saddle River, NJ: Pearson Prentice Hall.